

Software-hardware Integration and Human-centered Benchmarking for Socially-compliant Robot Navigation

Iaroslav Okunovich¹, Vincent Hilaire¹, Stephane Galland¹, Olivier Lamotte¹,
 Liubov Shilova², Yassine Ruichek¹, and Zhi Yan^{1*}

Abstract—The social compatibility (SC) is one of the most important parameters for service robots. It characterises the interaction quality between a robot and a human. In this paper, we first introduce an open-source software-hardware integration scheme for socially-compliant robot navigation and then propose a human-centered benchmarking framework. For the former, we integrate one 3D lidar, one 2D lidar, and four RGB-D cameras for robot exterior perception. The software system is entirely based on the Robot Operating System (ROS) with high modularity and fully deployed to the embedded hardware-based edge while running at a rate that exceeds the release frequency of sensor data. For the latter, we propose a new human-centered performance evaluation metric that can be used to measure SC quickly and efficiently. The values of this metric correlate with the results of the Godspeed questionnaire, which is believed to be a golden standard approach for SC measurements. Together with other commonly used metrics, we benchmark two open-source socially-compliant robot navigation methods, in an end-to-end manner. We clarify all aspects of the benchmarking to ensure the reproducibility of the experiments. We also show that the proposed new metric can provide further justification for the selection of numerical metrics (objective) from a human perspective (subjective).

I. INTRODUCTION

The development of computing and sensing technologies allows to apply mobile robotic systems in different environments. Robot behavior is especially important in an environment with human presence, such as in the case of mobile robots for logistic [1], [2] or disinfection [3] purposes. Although the robot systems perform relatively well, people still tend to fear of them, which negatively affects mental health and decreases the productivity of the workers [4]. The general problem behind the fear is a lack of understanding of robot's behavior [5]. If a person cannot predict the behavior of a robot, they prefer to avoid working with it. The intelligence of robots is different from that of human beings, and the robot-human interaction is limited in ways of communication compared to human-human interaction. People feel safer in the presence of other people, thus preferring them to robots as their working partners. The safety feeling comes from the belief that people's behavior is more adequate and predictable. Similarly, one generally feels uneasy when communicating with a drunk person, as the alcohol makes their behavior unpredictable.

This work was supported by the Bourgogne-Franche-Comté regional research project LOST-CoRoNa.

¹CIAD UMR 7533, Univ. Bourgogne Franche-Comté, UTBM, F-90010 Belfort, France. firstname.lastname@utbm.fr

²Center for Bioinformatics, Saarland Informatics Campus, Saarbrücken, Germany. lish00001@stud.uni-saarland.de

*Corresponding Author.



Fig. 1. The experiment to examine the social compatibility of robot navigation. The person makes an action in the room, while the mobile robot moves near the person. The logistic operations at a warehouse are an example of a real scenario, where the human and mobile robot collaborate.

To make the behavior of the robot more understandable, one could apply different technical solutions. In addition to the necessary sensors to perceive the world, the robot can be equipped with additional mechanical elements to show its behavior or intention. The light [6] and sound [7] signaling system can be applied to show the people around when the robot is going to change the direction of the movement. Also, additional screen [8] can be applied for this purpose. However, there is currently a lack of open-source software-hardware integration solutions, which is not conducive to the community's further exploration of the overall performance of the robotic system.

Another way to decrease the fear of robots is to improve the quality of navigation algorithms. This implies, that the robot tries to follow unspoken social rules which people have in their regular life. For instance, the left and right-hand rules for collision avoidance [9], social zones around the people [10] and navigation through the pedestrian flow [11]. However, developing a metric to measure SC is problematic. To demonstrate the quality of the social part of the developed navigation method the robot-centered numerical metrics

(RCM) are applied in many studies [9], [10]. As fear is not a numerical parameter, scientists also need to use metrics from psychology to assess the acceptance (compatibility from a robot perspective) of the robot by people. One of the most popular approaches is to invite people to participate in an experiment (such as that shown in Fig. 1) and then conduct a questionnaire to the participants. However, different papers apply different metrics and experimental settings to measure the impact of robots on humans, while often, reproducing these experiments is not straightforward, making comparisons between different methods tricky.

The contributions of this paper are twofold.

- We present a software-hardware integration scheme, in which the hardware includes an off-the-shelf robot and sensors, allowing to create an affordable setup that can be easily reproduced both physically and in simulation, while the software system is entirely based on ROS, with high modularity, fully deployed to the embedded hardware of the robot being capable of running at a rate that exceeds the frequency with which sensor data is published, and publicly available to the community¹.
- We propose an end-to-end human-centered benchmarking framework that incorporates a new human-centered metric (HCM). We benchmark two open-source methods under the proposed framework. All experimental settings and parameters are clearly stated to ensure the reproducibility of the experiments. Furthermore, our insights into the experimental results reveal that the proposed new metric can be used for further correlation analysis on numerical ones.

II. RELATED WORK

Software-hardware integration for robot systems usually follows a similar principle, but the specific integration methods are different according to the development level of software and hardware at that time. Early integration focuses on overall system availability [12]. Later, with the development of technology, functionality was considered more in the integration, for example, the system integration of a mobile manipulator was introduced in [13]. In recent years, researchers have paid increasing attention to the reliability, flexibility, real-time, etc. of the integrated systems [14].

Much work has been done on socially-aware robot navigation and interaction between humans and autonomous mobile robots. However, the applied experiment conditions (hardware, software, environment, etc.) and metrics to measure method performance vary from paper to paper significantly. Chen *et al.* [9] focused on a multiagent collision avoidance algorithm that exhibits socially-compliant behavior. The authors trained their algorithm in a reinforcement learning framework and compared it with two algorithms in simulation. They chose three performance metrics: 1) average extra time to reach the goal; 2) minimum separation distance to other agents; 3) relative preference between left-handedness and right-handedness. Although the experiment in real life

proved that the developed method was safe, the work did not show the opinion of the people about the behavior of the robot. David *et al.* [15] compared standard and social navigation strategies for efficient robot behavior. For a person and a robot moving in the corridor, the following metrics were recorded: 1) the speed of the robot and the person during the experiment. Higher speed indicated more efficient human-robot interaction (HRI). It was shown to be a useful metric to measure the difference in HRI representing the changing human behavior; 2) the signaling distance between the person and the robot. For the human, it was measured when the person started to change their trajectory to react to the robot. For the robot, it was measured when the robot started to avoid the person. This metric was shown to be suitable for a perception system, but not for HRI.

Bartneck *et al.* [16] developed the standardized measurement questionnaire for HRI with 29 questions, which assess the perception of robots by humans. The answers were scaled from 1 to 5 with 1 being the worst and 5 being the best opinion mark. The questions were divided into 5 groups: anthropomorphism, animacy, likeability, perceived intelligence, and perceived safety. This questionnaire is currently used as a baseline of numerous questionnaires in HRI research [17]. However, the metric leads to limited autonomy. A robot itself cannot assess it, i.e. the metric does not correspond to RCM. Mavrogiannis *et al.* [17] presented the user study design for the experimental evaluation of mobile robot navigation strategies in human environments. The authors applied different types of metrics to define the more suitable navigation strategies for HRI, such as average acceleration and energy, minimum robot-human distance, path irregularity, path efficiency, time spent per unit path length, and topological complexity. After the experiment, the participants evaluated HRI during the experiment through a questionnaire. The combination of the results of two different types of metrics allowed to measure the HRI by RCM and confirmed the results through comparison with the questionnaire answers.

Through our investigation, we found that there is still a lot of room for exploration in terms of software-hardware integration and benchmarking methods. For the former, although there are some open-source modules, complete open-source systems, including instrumented CAD designs, 3D models of sensor mounts, perception and decision-making software modules, are rare. In addition, overall software systems optimized for edge hardware are even rarer. For the latter, the existing SC navigation evaluation mainly uses RCM, and a small amount of work draws on the questionnaire form of the HRI community, but a large number of questions lack experimental efficiency and the relevance of some questions is questionable. Furthermore, the lack of necessary experimental information makes the community's benchmarking becomes difficult. The status quo drives us to develop not only reusable robotic systems, but also reproducible experiments based on standardizable processes to accelerate relevant method development and comparison in our community.

¹https://github.com/Nedzhaken/human_aware_navigation

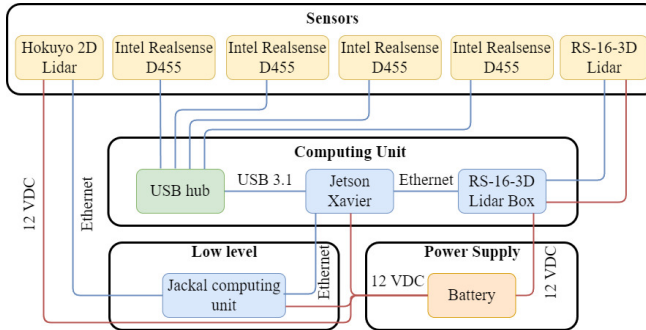


Fig. 2. The system configuration of the instrumented robot.

III. SOFTWARE-HARDWARE INTEGRATION

Typical software-hardware integration for robot systems includes four aspects: hardware, sensors, communications and software. Fig. 2 and Fig. 3 give an intuitive idea of the overall system we developed. Below we describe each aspect in detail.

A. Hardware

The robot chassis is a Clearpath Jackal UGV with an onboard Mini-ITX PC. This PC is dedicated to those tasks with real-time requirements such as robot motion control and communication with essential (high frequency) sensors such as wheel encoders, IMU, 2D lidar, etc. The chassis is powered by a 270 watt-hour lithium-ion battery pack, that also powers an additional computing unit and sensors, supporting approximately two hours of autonomy for the entire robotic system. The additional computing unit is a Nvidia Jetson AGX Xavier Developer Kit, providing GPU support, which is mainly used for data processing of computationally hungry sensors such as 3D lidar and RGB-D camera. A USB hub is placed in order to connect four RGB-D cameras. In addition, a mini-display is mounted on the robot, which is the most important component that allows human-robot interaction in our current design.

B. Sensors

Four wheel encoders and an IMU are integrated into the robot at the factory for proprioception. The selection of exteroceptive sensors mainly considers three aspects: 1) long-term robot autonomy, i.e., the perception system needs to be robust to various lighting conditions; 2) the largest possible range of perception, including breadth and depth, and best to avoid dead spots; 3) acquisition of semantic information of the environment, especially based on color and texture information. Obviously, a multimodal sensor system is needed. In our case, a 3D lidar, a 2D lidar, and four RGB-D cameras are integrated, and their specifications are shown in Table I.

The 2D lidar is mounted 30 cm above the ground, facing forward. Integrating this sensor instead of using a one-stop solution based on the 3D lidar is because its lower position is more in line with the needs of SLAM and navigation, and can further compensate for the blind spot of perception caused

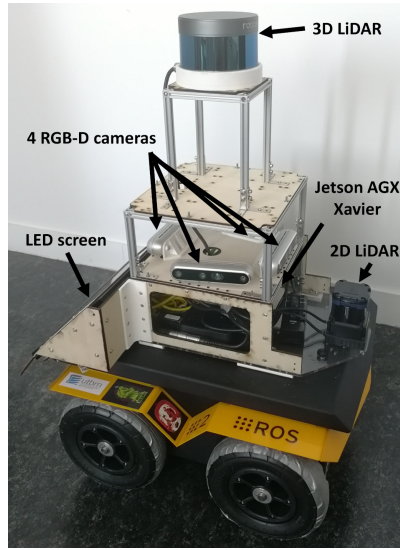


Fig. 3. The mobile platform with a developed perception system.

by 3D lidar due to its relatively high installation position. More importantly, using 2D lidar with higher measurement frequency, accuracy, and resolution than 3D lidar is beneficial for robot localization and collision-free navigation. In our case, a Hokuyo UTM-30LX-EW 2D lidar is used.

TABLE I
SPECIFICATIONS OF SENSORS

Specification / Sensor	RGB-D camera	3D lidar	2D lidar
Data release frequency, Hz	30	10	40
Measurement distance, m	6	150	30
Field-of-View (horizontal), °	87	360	270
Field-of-View (vertical), °	58	30	-

The 3D lidar (a Robosense RS-LiDAR-16) is mounted on top of the entire perception system, 80 cm above the ground. Like 2D lidar, the sensor in this modality is not sensitive to lighting conditions and is therefore suitable for day and night use. Moreover, since the 3D lidar typically has panoramic scanning capability and actual detection capability of up to tens of meters, the robot can detect humans or other dynamic objects as early as possible, and therefore have more time to react accordingly (e.g. timely adjusting its path) [18], [19]. The shortcoming of lidar is that it can only provide a set of sparse coordinate points, which is not enough to understand the environmental context. While some lidars provide intensity information, the value of the intensity is entirely determined by the lidar's internal signal processing unit, which is usually a black box (for commercial reasons) [20]. Therefore, it is necessary to add vision sensors.

Four Intel RealSense D455 RGB-D cameras are installed 32.7 cm from the ground and placed towards all sides of the robot for a quasi-panoramic view. And due to our requirements for the safety and sociality of the robot, the left and right cameras are slightly shifted to the front in order to close the blind spot of perception. Although these cameras are sensitive to lighting conditions, their ability to provide

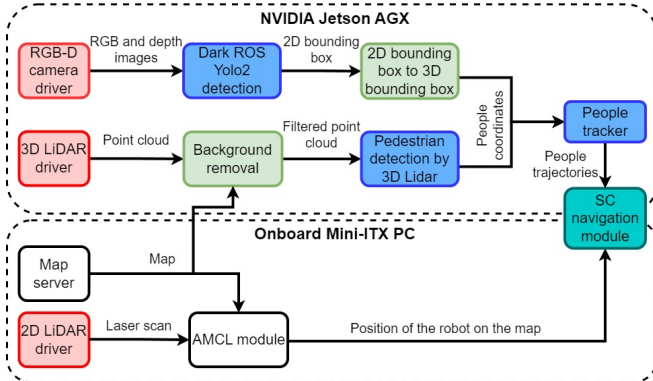


Fig. 4. Our current socially-compliant robot navigation software design. The red blocks refer to drivers, which are responsible for the sensory data representation. The blue blocks represent state-of-the-art methods. The light green blocks refer to the modules we developed. The white blocks represent the modules provided by the ROS navigation stack. The turquoise block represents the SC navigation module.

rich environmental semantics and reliable close-range object detection has made them a standard component in today's mobile robots.

C. Communications

Communications between all hardware components are based on wired connections. As a robotic system, the data transfer rate and communication bandwidth must be fully considered to avoid undue challenges to the algorithm's fault tolerance and to avoid catastrophic data delay and loss. Based on this principle, the 2D and 3D lidars are respectively connected to the on-board PC and Nvidia AGX through Ethernet cables to ensure that the sensory data is processed by the corresponding computing units (CPU or GPU) in time. The AGX and the robot's onboard PC are directly connected via an Ethernet cable and maintain soft time synchronization. Additionally, the four RGB-D cameras are connected to the Nvidia AGX via the USB hub.

D. Software

The software system has been fully implemented into ROS [21] with high modularity (see Fig. 4), and is publicly available to the community. It is divided into two parts, i.e., objectless navigation and human-aware perception, corresponding to the two computing units, i.e., the onboard PC and the Nvidia AGX, with loose coupling. The deployment of the SC module enjoys full flexibility under our software design, depending on its dependencies, it can be deployed either on the PC side or on the AGX side.

The human-aware perception is based on a tracking-by-detection pipeline. Specifically, we provide human detectors with two different modalities, image-based, and point cloud-based. The former uses off-the-shelf YOLOv2 [22] to first obtain the 2D bounding box (BB) of people from the RGB image, then utilizes the registered depth information to project the 2D BB to 3D, and finally calculates the 3D coordinates of the detected human (i.e. 3D BB centroid).

The latter utilizes the state-of-the-art AdaptiveClustering-SVM (GPU version) detector [23] to obtain the human 3D coordinates (i.e. 3D BB centroid) directly from the point cloud. In addition, in order to reduce false alarms, we specially developed a ROS package to remove background point clouds, which correspond to those occupied and unknown cells registered in the grid map. Then, an advanced multi-target tracking system is used and high-level information fusion is performed on detections from different detectors in a loose manner [24].

A typical SC navigation module needs to know the global position of the robot (e.g., in a map reference frame) and the absolute or relative positions and velocities of surrounding pedestrians, so as to reflect changes to the local map and adjust the robot's path planning in time. In our system, the pedestrian's speed is estimated by the tracker. Certainly, sensors such as millimeter-wave radar can also directly provide velocity information of objects.

Moreover, it is worth noting that our software system is fully deployed to the edge based on embedded devices and can run faster than the release frequency of sensor data. In particular, our pedestrian tracking system can operate at up to 20 Hz, which actually opens a door to potential industrial applications.

IV. BENCHMARKING FRAMEWORK

Benchmarking of HRIs is often very challenging. This is due on the one hand to the increasing complexity of the robotic system (both hardware and software) and, on the other hand, to the spontaneous behavior of different participants (especially non-robotics practitioners) with different understandings of the experimental procedures, making benchmarks difficult to reproduce. To this end, we propose an end-to-end benchmarking framework, emphasizing human-centricity, that enables rapid and efficient evaluation and comparison of the performance of different SC navigation methods, by clearly defining experimental scenarios and evaluation metrics. Moreover, we propose to divide the experiment into as explicit and small steps as possible, ideally consisting of simple motion or action primitives, which both make the experiment easier to reproduce and avoid any ambiguity. For example, the instruction to a person could be "walk three meters forward in a straight line" rather than "walk around the room for 10 seconds". Based on this principle, we propose the following experimental design.

A. Experiment Design

Unlike the no-object experiments commonly seen in the literature, our experiment required humans to move cartons. In this manner, we tried to reproduce the situation in which a person should complete a working task in presence of the robot. Our understanding is that people are less likely to pay attention to the robot, while they are concentrated on their tasks [25]. Thus, this experiment setting should provide more reliable and realistic results for the SC evaluation. Specifically, in a 2.5×4 m room, trial participants were asked to carry three cartons from one side of the room to the other

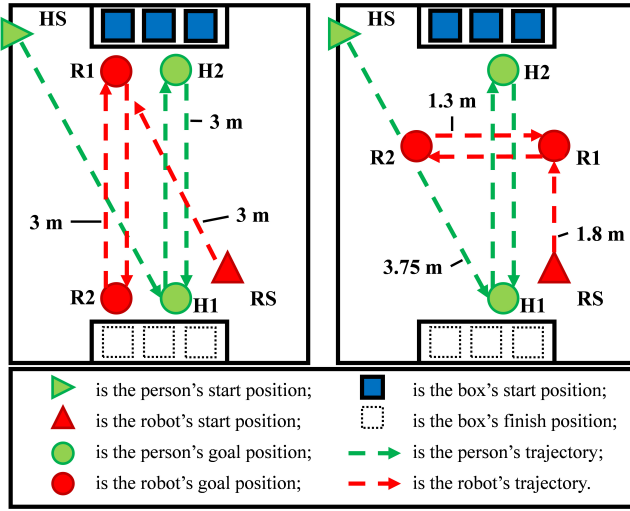


Fig. 5. Our reproducible experiment design. Shown on the left is the case where the robot moves parallel to the direction of the pedestrian. Shown on the right is the case where the robot moves perpendicular to the pedestrian.

(see Fig. 5). During this time, the robot will move in the shared space. The acceleration and maximum velocity of the robot are set to 0.3 m/s^2 and 0.3 m/s , respectively. Humans are told to move at normal speed. The evaluation of the SC navigation methods consists of two parts, the path of the robot is parallel or perpendicular to the pedestrian. To make our experiments reproducible and to facilitate the comparison of results between different methods, we next describe the full implementation details.

The initial position of the pedestrian is at the entrance of the room, denoted as HS. The person is asked to first reach H1 and then H2, walking in a straight line. Upon reaching H2, pedestrians should pick up a carton box and take it to H1 to drop it off. This process is repeated until all cartons were transported to H1 and the experiment ends. On the other side, the starting position of the robot is at the opposite corner of the room entrance, marked RS. Similarly, the robot will first move to R1, and then go back and forth between R1 and R2 four times to ensure that the pedestrian completes the task within its moving time. As shown in Fig. 5, the robot moves with R1-R2 parallel or perpendicular to H1-H2. When the robot finally reached R1, we collect the experimental metrics.

B. Human-centered Metrics

To evaluate navigation systems that conform to social norms, we argue that in addition to conventional RCM, metrics that conform to the expectations of human participants should be developed, as this will reflect their subjective feelings about the robot's behavior. To this end, we select 12 most appropriate questions from the classic Godspeed questionnaire² [16], each of which is answered on a scale of 1 to 5. Furthermore, although fine-grained questions can provide the basis for microscopic analysis of SC navigation performance, direct questioning would be a more reliable

way to assess human receptivity to robot social navigation. While the latter is particularly effective in a large-scale survey, as people only need to answer one question. We, therefore, propose a new question, i.e., “Could you rate the general behavior of the agent?”, and the answer to it is always on a 5-point scale, with 1 for “I do not accept the agent's behavior” and 5 for “I accept the agent's behavior”.

C. Numerical Metrics

We carefully select five commonly used numerical metrics from the literature and additionally propose a dual metric among them. Insights into the SC correlations of these metrics will be given in Section V-B.

1) *The robot extra time ratio* evaluates how efficiently a robot can complete a task in an environment shared with humans [9], [26], [27], which is defined as:

$$R_{extra}^r = T^r / T_h^r \quad (1)$$

where T^r and T_h^r are the time required for the robot to complete the task without and with the presence of humans, respectively.

2) *The human extra time ratio* is a dual of the previous one, first proposed in this paper, to assess changes in human performance when working with robots. It can help us better understand the connection between human performance and SC, which is defined as:

$$R_{extra}^h = T^h / T_r^h \quad (2)$$

where T^h and T_r^h are the time it takes for a human to complete the task without and with the presence of robots, respectively.

3) *The extra distance ratio* evaluates system performance in terms of the distance a robot would have to travel additionally when a human is present [28], [17], which is defined as:

$$R_{dist} = D^r / D_h^r \quad (3)$$

where D^r and D_h^r represent the distance the robot traveled to complete a task with and without the presence of a human, respectively.

4) *The success ratio* assesses the ability of a robot to complete a task without colliding with a human [9], [26], [27], which is defined as:

$$R_{succ} = N_{succ} / N \quad (4)$$

where N_{succ} represents the number of successful trials where the robot does not hit a human, and N indicates the total number of trials.

5) *The hazard ratio* assesses the time a robot gets too close to a human [27], which is defined as:

$$R_{haza} = \frac{1}{n} \cdot \sum_{i=1}^n \frac{T_i^{hazard}}{T_i^{social}} \quad (5)$$

where n is the number of people, T_i^{hazard} is the duration of time when the distance between the robot and the i -th person is less than the safe distance (denoted as D_{safe}), and T_i^{social} is the duration of the time when the distance between

²https://github.com/Nedzhaken/human_aware_navigation

the robot and the i -th person is less than the social distance (denoted as D_{social}). In our experiments, $D_{safe} = 0.2\text{ m}$ and $D_{social} = 0.4\text{ m}$.

6) *The deceleration ratio* evaluates a robot's ability to slow down when approaching a human [15], which is defined as:

$$R_{dec} = \frac{1}{n} \cdot \sum_{i=1}^n \frac{V_i}{V^{max}}, \quad (6)$$

where n represents the number of speed measurements when the robot is less than D_{social} from the human. V_i represents the instantaneous speed of the robot at i -th measurement, and V^{max} is the maximum velocity of the robot (i.e. 0.3 m/s).

V. EXPERIMENTS

Our experiments aim to benchmark two open-source SC navigation methods, on the one hand to show the deployability and flexibility of the integrated software-hardware robotic system, in which the SC navigation module is designed as a plug-and-play component, and on the other hand to show the effectiveness of the proposed benchmarking framework. Furthermore, we reveal how to examine numerical metrics with HCM to explore the experimental relevance of the former.

A. Evaluated Methods

We attempted to deploy several open-source methods, and finally report the results of two of them in this paper, based on: 1) the method must be deployable on real robots, and 2) the effectiveness of the method must be confirmed in its corresponding paper.

- *Social Navigation Layers (SNL)*³ [29]: It implements a Gaussian Mixture Model (GMM) around the detected person on the navigation cost map. The extra cost area around the person makes the robot consider avoiding it when planning its path. This allows the robot to exhibit better social attributes during navigation. In our experiments, due to site constraints, the social radius was set to be 0.4 m centered on the person. Also, if the person moves, the social area grows in the direction of the movement (i.e., from a circle to an ellipse).
- *Time Dependent Planning (TDP)*⁴ [30]: This method is similar to SNL, except that the social area is no longer limited to a person's current location, but also includes his or her predicted location several time steps in the future (i.e., based on a constant velocity model).

Additionally, three baseline methods are incorporated.

- *Collision Avoidance with Deep Reinforcement Learning (CADRL)*⁵: This method is the underlying implementation of the well-known SA-CADRL (socially-aware CADRL) [26], while the latter has not been ROSified. However, it is still considered a baseline, as collision avoidance is one of the most fundamental elements in the social properties of robot navigation.

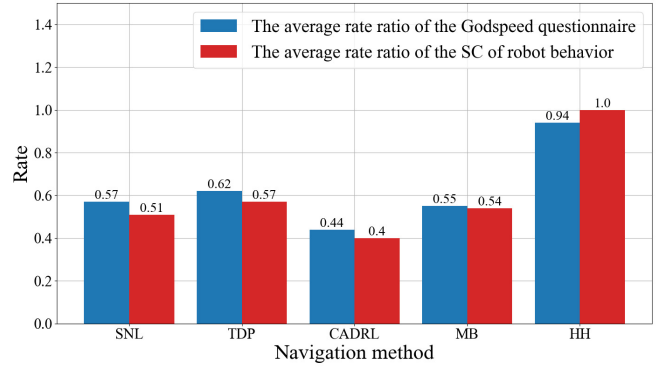


Fig. 6. The results of the 12 Godspeed questionnaire (in blue) and our new question (in red, named as SC of robot behavior), normalized to $[0, 1]$.

- *move_base (MB)*⁶: This is a basic component provided by ROS navigation stack and does not contain any SC modules.
- *Human-human interaction (HH)*: In this case, the robot is replaced by a human who performs the task assigned to the robot (i.e., moving from one point to another).

Results based on numerical metrics were recorded during the execution of the above methods involving the robot, while participants were asked to fill out the questionnaire (13 questions in total) after all methods were performed. It should also be noted that our experiments focus on benchmarking of SC navigation rather than multi-sensor fusion, thus a forward-looking RGB-D camera is sufficient for human detection.

B. Experimental Results

Seven members from our lab participated in the experiment, three of whom have experience with mobile robots and others do not, which maximizes the unbiasedness of the experiment. Fig. 6 summarizes the normalized results based on the HCMs, where the blue bars represent the average rates for the 12 questions in the Godspeed questionnaire, while the red bars show the average rates for the new question we asked. Although the two presented similar results overall, we still peeked into diametrically opposed differences between HH and other methods. This finding is very encouraging as it reflects that traditional indirect fine-grained questions are likely to overly reflect a human acceptance of SC robot navigation. Moreover, the fact that HH scores in all questionnaires are much higher than other robot-based methods indicates that the current participants are not ready to coexist with robots, which may provide some reference for the roboethics community. In addition, TDP performs best in experiments involving the robot, which is reasonable since this method is the only one with pedestrian prediction capability, thus also confirming the importance of robot foresight in SC navigation.

The SC evaluation correlation of numerical metrics can be further analyzed using our new question. Table II shows

³https://github.com/DLu/navigation_layers

⁴https://github.com/marinaKollmitz/human_aware_navigation

⁵https://github.com/mit-acl/cadrl_ros

⁶<https://github.com/ros-planning/navigation>

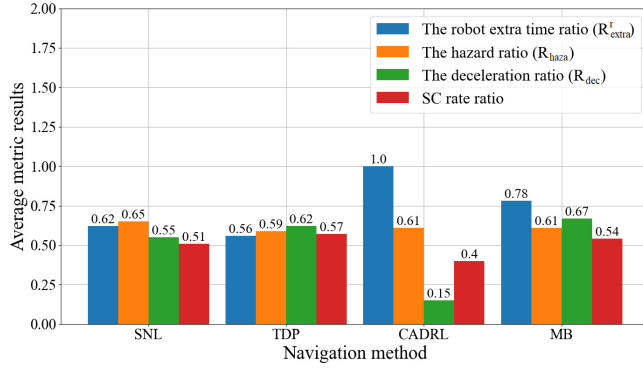


Fig. 7. The three numerical metrics most correlated with our new HCM.

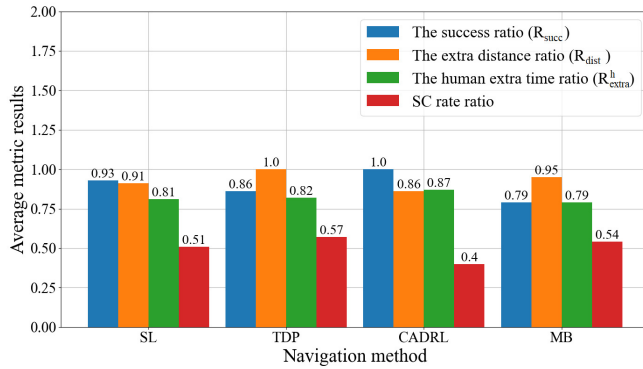


Fig. 8. The three numerical metrics least correlated with our new HCM.

these results, from most relevant on the left to least relevant on the right. The specific results for each method involving the robot are shown in Fig. 7 and Fig. 8, respectively.

TABLE II
CORRELATION OF THE NUMERICAL METRICS TO SC

Metric	R_{dec}	R^r_{extra}	R_{haza}	R_{dist}	R^h_{extra}	R_{succ}
Correlation	0.355	0.282	-0.157	-0.090	-0.049	0.024

Above all metrics, the deceleration ratio R_{dec} is the closest to the SC rate in regard to trend. The velocity decreases in the proximity of people, as the robot freezes during the attempts to avoid the person. The social zones of the SL and TDP algorithms improved the SC of the methods, but they also created additional limitations to the robot's speed. The robot with MB algorithm reacts to the person's presence at a very close distance. Sometimes the lack of reaction to the person allows the robot to move without slowing down. Thus, the MB demonstrates the highest deceleration ratio. The robot extra time ratio R^r_{extra} has an inverse relationship to the SC rate. Better social navigation methods require more time for the robot to complete the task. The high negative correlation allows to use the metric for the SC measurement in the future. The hazard ratio R_{haza} does not differ significantly depending on the methods and amounts to around 0.6. Even though this metric shows some correlation with SC, in the current configuration it cannot be used as the main numerical

metric in SC assessment. The result of the hazard ratio shows that the correlation without analysis cannot be the criteria to choose the most suitable numerical metric.

The extra distance ratio R_{dist} demonstrates the same trend as the SC, with the highest values in the TDP method and the lowest values in CARDL. Thus, the extra distance and extra time have different tendencies. Spending more time on the task does not lead to the increase of the robot's path. When avoiding people the robot spends the most time in a freezing state or rotation around the current position. The success ratio R_{succ} has the lowest correlation value with the SC. The plot in Fig. 8 shows that the robot with the CADRL method does not touch people during the experiment. At the same time, the CADRL method has the lowest SC rate. Thus, this metric could be applied only as a secondary metric. The human extra time ratio R^h_{extra} shows that the robot increases the time that a person needs to solve the task. The value of this metric is growing with each next experiment. This result could be explained with two assumptions. The metrics depend on the different robot's navigation strategies. Or the person learns the general pattern of the robot's movements and spends less time to react to the robot in each new experiment. The results of our experiment could not be applied to choose a valid assumption. We would not suggest to apply this metric as the main metric of SC.

In summary:

- HH interaction has higher SC than HRI.
- When people work with robots, they need more time to complete their tasks. But productivity returns over time as humans learn about robot behavior.
- The direct question about robot SC behavior can be an alternative to the fine-grained ones.
- The deceleration, extra distance, and extra robot time ratios can be used as priority numerical metrics to measure SC. Others can be used as auxiliary metrics.

VI. CONCLUSIONS

In this paper, we proposed a software-hardware integration and a human-centered benchmarking framework for socially-compliant robot navigation, and benchmarked two open-source approaches with the developed robot prototype. Our ROS-based software and instrumentation design are publicly available to the community. The benchmarking framework is end-to-end and explicitly provides all parameters required for the reproduction of experimental results. Our future work will delve into new approaches to SC navigation and keep evaluating them under our benchmarking framework. Furthermore, we will develop dependency functions for SC results from the three most relevant numerical metrics. This task can be done by using neural networks, but more training data needs to be collected.

ACKNOWLEDGMENT

We thank RoboSense for sponsoring us with a RS-16 lidar, UTBM CRUNCH Lab for their support in robotic instrumentation, as well as all colleagues involved in the experiments.

REFERENCES

[1] R. Fukui, Y. Yamada, K. Mitsudome, K. Sano, and S. Warisawa, "Hangrawler: Large-payload and high-speed ceiling mobile robot using crawler," *IEEE Transactions on Robotics*, vol. 36, no. 4, pp. 1053–1066, 2020.

[2] J. Baćk, P. Tkáč, L. Hric, S. Alexovič, K. Kyslan, R. Olexa, and D. Perduková, "Phollower—the universal autonomous mobile robot for industry and civil environments with covid-19 germicide addon meeting safety requirements," *Applied Sciences*, vol. 10, no. 21, p. 7682, 2020.

[3] S. Perminov, N. Mikhailovskiy, A. Sedunin, I. Okunovich, I. Kalinov, M. Kurenkov, and D. Tsetserukou, "Ultrabot: Autonomous mobile robot for indoor uv-c disinfection," in *2021 IEEE 17th International Conference on Automation Science and Engineering (CASE)*. IEEE, 2021, pp. 2147–2152.

[4] M. Sahin and C. Savur, "Evaluation of human perceived safety during hrc task using multiple data collection methods," in *2022 17th Annual System of Systems Engineering Conference (SOSE)*. IEEE, 2022, pp. 465–470.

[5] N. Akalin, A. Kristoffersson, and A. Loutfi, "Do you feel safe with your robot? factors influencing perceived safety in human-robot interaction based on subjective and objective measures," *International journal of human-computer studies*, vol. 158, p. 102744, 2022.

[6] R. Fernandez, N. John, S. Kirmani, J. Hart, J. Sinapov, and P. Stone, "Passive demonstrations of light-based robot signals for improved human interpretability," in *2018 27th IEEE International Symposium on Robot and Human Interactive Communication (RO-MAN)*. IEEE, 2018, pp. 234–239.

[7] M. C. Shrestha, T. Onishi, A. Kobayashi, M. Kamezaki, and S. Sugano, "Communicating directional intent in robot navigation using projection indicators," in *2018 27th IEEE International Symposium on Robot and Human Interactive Communication (RO-MAN)*. IEEE, 2018, pp. 746–751.

[8] J. Hart, R. Mirsky, X. Xiao, S. Tejeda, B. Mahajan, J. Goo, K. Baldauf, S. Owen, and P. Stone, "Using human-inspired signals to disambiguate navigational intentions," in *International Conference on Social Robotics*. Springer, 2020, pp. 320–331.

[9] Y. F. Chen, M. Everett, M. Liu, and J. P. How, "Socially aware motion planning with deep reinforcement learning," in *2017 IEEE/RSJ International Conference on Intelligent Robots and Systems (IROS)*. IEEE, 2017, pp. 1343–1350.

[10] X.-T. Truong and T.-D. Ngo, "Dynamic social zone based mobile robot navigation for human comfortable safety in social environments," *International Journal of Social Robotics*, vol. 8, no. 5, pp. 663–684, 2016.

[11] Y. Morales, N. Akai, and H. Murase, "Personal mobility vehicle autonomous navigation through pedestrian flow: A data driven approach for parameter extraction," in *2018 IEEE/RSJ International Conference on Intelligent Robots and Systems (IROS)*. IEEE, 2018, pp. 3438–3444.

[12] H. Shin, K. Kon, H. Igarashi, Y. Anbe, K. Kim, S. Hanamoto, R. Yamasaki, S. Toyoshima, N. Sato, T. Kamegawa *et al.*, "Hardware-software integration of a practical mobile robot platform," in *2011 IEEE/SICE International Symposium on System Integration (SII)*. IEEE, 2011, pp. 1263–1268.

[13] A. Bubeck, F. Weisshardt, T. Sing, U. Reiser, M. Hägele, and A. Verl, "Implementing best practices for systems integration and distributed software development in service robotics—the care-o-bot® robot family," in *2012 IEEE/SICE International Symposium on System Integration (SII)*. IEEE, 2012, pp. 609–614.

[14] Z. Yan, S. Schreiberhuber, G. Halmetschlager, T. Duckett, M. Vincze, and N. Bellotto, "Robot perception of static and dynamic objects with an autonomous floor scrubber," *Intelligent Service Robotics*, vol. 13, no. 3, pp. 403–417, 2020.

[15] D. V. Lu and W. D. Smart, "Towards more efficient navigation for robots and humans," in *2013 IEEE/RSJ International Conference on Intelligent Robots and Systems*. IEEE, 2013, pp. 1707–1713.

[16] C. Bartneck, D. Kulić, E. Croft, and S. Zoghbi, "Measurement instruments for the anthropomorphism, animacy, likeability, perceived intelligence, and perceived safety of robots," *International journal of social robotics*, vol. 1, no. 1, pp. 71–81, 2009.

[17] C. Mavrogiannis, A. M. Hutchinson, J. Macdonald, P. Alves-Oliveira, and R. A. Knepper, "Effects of distinct robot navigation strategies on human behavior in a crowded environment," in *2019 14th ACM/IEEE International Conference on Human-Robot Interaction (HRI)*. IEEE, 2019, pp. 421–430.

[18] Z. Yan, T. Duckett, and N. Bellotto, "Online learning for human classification in 3d lidar-based tracking," in *2017 IEEE/RSJ International Conference on Intelligent Robots and Systems (IROS)*. IEEE, 2017, pp. 864–871.

[19] L. Sun, Z. Yan, S. M. Mellado, M. Hanheide, and T. Duckett, "3dof pedestrian trajectory prediction learned from long-term autonomous mobile robot deployment data," in *2018 IEEE International Conference on Robotics and Automation (ICRA)*. IEEE, 2018, pp. 5942–5948.

[20] T. Yang, Y. Li, Y. Ruichek, and Z. Yan, "Performance modeling a near-infrared tof lidar under fog: A data-driven approach," *IEEE Transactions on Intelligent Transportation Systems*, vol. 23, no. 8, pp. 11227–11236, 2022.

[21] S. Gatesichapakorn, J. Takamatsu, and M. Ruchanurucks, "Ros based autonomous mobile robot navigation using 2d lidar and rgb-d camera," in *2019 First international symposium on instrumentation, control, artificial intelligence, and robotics (ICA-SYMP)*. IEEE, 2019, pp. 151–154.

[22] J. Redmon and A. Farhadi, "Yolo9000: better, faster, stronger," in *Proceedings of the IEEE conference on computer vision and pattern recognition*, 2017, pp. 7263–7271.

[23] T. Yang, Y. Li, C. Zhao, D. Yao, G. Chen, L. Sun, T. Krajník, and Z. Yan, "3d tof lidar in mobile robotics: A review," *CoRR*, vol. abs/2202.11025, 2022.

[24] Z. Yan, T. Duckett, and N. Bellotto, "Online learning for 3d lidar-based human detection: experimental analysis of point cloud clustering and classification methods," *Autonomous Robots*, vol. 44, no. 2, pp. 147–164, 2020.

[25] R. Y.-T. Lo, M.-W. Suen *et al.*, "The influence of visual distraction on awareness test," *Sociology Mind*, vol. 4, no. 04, p. 259, 2014.

[26] M. Everett, Y. F. Chen, and J. P. How, "Motion planning among dynamic, decision-making agents with deep reinforcement learning," in *2018 IEEE/RSJ International Conference on Intelligent Robots and Systems (IROS)*. IEEE, 2018, pp. 3052–3059.

[27] L. Liu, D. Dugas, G. Cesari, R. Siegwart, and R. Dubé, "Robot navigation in crowded environments using deep reinforcement learning," in *2020 IEEE/RSJ International Conference on Intelligent Robots and Systems (IROS)*. IEEE, 2020, pp. 5671–5677.

[28] Y. Gao and C.-M. Huang, "Evaluation of socially-aware robot navigation," *Frontiers in Robotics and AI*, p. 420, 2021.

[29] D. V. Lu, D. Hershberger, and W. D. Smart, "Layered costmaps for context-sensitive navigation," in *2014 IEEE/RSJ International Conference on Intelligent Robots and Systems*. IEEE, 2014, pp. 709–715.

[30] M. Kollmitz, K. Hsiao, J. Gaa, and W. Burgard, "Time dependent planning on a layered social cost map for human-aware robot navigation," in *2015 European Conference on Mobile Robots (ECMR)*. IEEE, 2015, pp. 1–6.